

Interband Transitions in Ultrathin GaAs-AlAs Superlattices

M. Alouani, S. Gopalan, M. Garriga, and N. E. Christensen

Max-Planck-Institut für Festkörperforschung, Postfach 80 06 65, D-7000 Stuttgart 80, Federal Republic of Germany
(Received 1 June 1988)

Experimental as well as theoretical data for the optical properties of ultrathin GaAs-AlAs (001) superlattices are presented and analyzed. The dielectric functions $\epsilon_1(\omega)$ and $\epsilon_2(\omega)$ are calculated by means of the linear muffin-tin-orbital method, whereas the experimental data are obtained by means of ellipsometry. Theory and experiments agree with respect to the structures in ϵ_2 and their variation in spectral position with superlattice period. Two structures specific to the superlattice are identified and explained in terms of the reduced symmetry as compared to the bulk materials. Variation of the polarization of the light is predicted to influence the optical properties only slightly.

PACS numbers: 73.20.Dx, 78.65.Fa

Short-period superlattices (SL's) consisting of alternating very thin (a few monolayers) layers of compound semiconductors may be considered as new, manmade, crystals that in general have physical properties different from those of the constituents in their bulk form, or of their alloys. It is of general interest to examine how the optical properties are influenced by the presence of the new periodicity along the SL growth direction. This has been demonstrated, for example, in the recent measurements¹ of the dielectric functions by means of spectroscopic ellipsometry. In this Letter we present results of *ab initio* calculations of the dielectric functions of one of the experimentally most widely studied systems, $(\text{GaAs})_m(\text{AlAs})_n$ SL's grown in the (001) direction. Several structures are identified, and their shifts in energy with the period [specified by (m,n)] of the SL discussed. This analysis emphasizes the effects of zone-folded bands and the quantum confinement of electronic states. The anisotropy effect is examined by our comparing $\epsilon_2^\perp(\omega)$ and $\epsilon_2^\parallel(\omega)$, for light polarized perpendicular and parallel, respectively, to the growth direction, and by our calculating the static dielectric constants ϵ_0^\perp and ϵ_0^\parallel . The experimental work of Ref. 1 considered SL's with $m=n$, but for a detailed analysis of the dependence of the optical properties on the composition, it is important to include also SL's with different GaAs and AlAs layer thicknesses. Therefore, new measurements have been performed for such systems, and some of the results are presented here.

To our knowledge, no theoretical study of the dielectric functions of ultrathin $(\text{GaAs})_m(\text{AlAs})_n$ SL's with $(m,n) > (1,1)$, which simultaneously covers the entire photon-energy range where all the optical structures are present, has been published. Caruthers and Lin-Chung² used an empirical pseudopotential method to derive band structures and dielectric functions, $\epsilon_2^\parallel(\omega)$ and $\epsilon_2^\perp(\omega)$, for the (1,1) SL. However, the bands derived in this way depend strongly on how the pseudopotentials are chosen, and the calculated² $\epsilon_2^\perp(\omega)$ is not consistent with ellipsometry measurements. Further, $\epsilon_2^\perp(\omega)$ and $\epsilon_2^\parallel(\omega)$ of

Ref. 2 differ considerably. This is particularly surprising as the lengths and strengths of the Ga-As and Al-As bonds are very similar, and hence only small polarization effects are expected. Kamimura and Nakayama³ used the pseudopotential method in conjunction with the $X\alpha$ method, with α adjusted so that the gaps of the constituents were close to the experimental values, to study $\epsilon_2(\omega)$ in the vicinity of the absorption edges ($\hbar\omega \leq 2.3$ eV).

Here the self-consistent scalar⁴ relativistic linear muffin-tin-orbital method⁵ is used in conjunction with the local-density approximation formalism⁶ to obtain the band structures of $(\text{GaAs})_m(\text{AlAs})_n$. As usual (see, for example, Christensen⁷) the application of the linear muffin-tin-orbital method to these rather open structures requires the introduction of "empty spheres." Also, the Ga-3d states are treated as fully relaxed band states. The importance of this is discussed elsewhere.⁸ In order to correct for the well-known "gap problem" that occurs when the local-density approximation is applied to semiconductors, we have added external potentials that are sharply peaked at the atomic sites, and that have strengths chosen⁷ such that the band gaps in bulk GaAs and AlAs at three symmetry points (Γ , X , and L) agree with experiments at 4 K. The SL potentials are then obtained by our iterating to self-consistency in the SL geometry, including these extra potentials without further parameter adjustment.

The dielectric functions are calculated with inclusion of the matrix elements $\langle n\mathbf{k} | P_j | n'\mathbf{k} \rangle$. There are evaluated⁹ for each component, $P_j = (\hbar/i)\partial_j$, of the momentum operator \mathbf{P} ($j=x$ or y and z), with the wave function $|n\mathbf{k}\rangle$ expressed in terms of the one-center expansion.⁵ The \mathbf{k} -space integration is performed with use of the tetrahedron method¹⁰ based on 330 \mathbf{k} points in the irreducible part of the tetragonal Brillouin zone (BZ).

The calculated $\epsilon_2^\perp(\omega)$ for $(m,n)=(2,1)$ (the spectra for other cases will be presented in Ref. 11) is shown in Fig. 1, where it is compared to the experimental spectrum obtained by ellipsometry. The measurements were

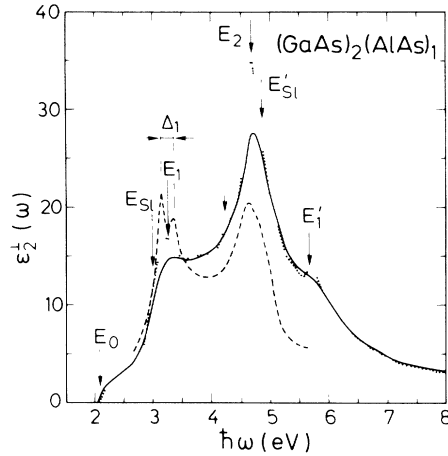


FIG. 1. Imaginary part, $\epsilon_2''(\omega)$, of the dielectric function of the $(\text{GaAs})_2(\text{AlAs})_1$ superlattice. The full-line curve differs from the calculated (dotted) $\epsilon_2''(\omega)$ function by inclusion of a lifetime broadening (simulated by our folding with a Lorentzian of 0.10 eV FWHM). The dashed curve shows the experimental results obtained with ellipsometry.

done on 0.4- μm -thick samples grown on GaAs substrates by molecular-beam epitaxy. Because of the large refractive index of the materials, the electric field in the sample is polarized mainly perpendicular to the growth direction. The measured dielectric function therefore corresponds to $\epsilon_2^\perp(\omega)$. No experimental data exist with which we could compare our calculations for parallel polarization. The spectra are therefore not included here (they will be shown elsewhere, Ref. 11). The spectrum

shown with a full line in Fig. 1 differs from the calculated dotted curve by inclusion of a lifetime broadening, simulated by folding with a Lorentzian of 0.10 eV FWHM. The positions of all⁴ the peaks in $\epsilon_2^\perp(\omega)$ are given in Table I, and compared to data obtained, experimentally in the present work as well as those presented elsewhere.^{1,12,15-18} In the same table we also give the peak positions of bulk GaAs and AlAs. The experimental energies were obtained from a fit of critical-point line-shape functions to the numerical second derivative of the spectra.

The electronic properties of GaAs and AlAs are very similar, and therefore only small differences are expected between bulk and SL band structures. This is demonstrated¹¹ by our reproducing the band structures and dielectric functions of bulk GaAs as $(\text{GaAs})_2$ or $(\text{GaAs})_3$ SL's. The changes in the band structure due to the substitution of one Ga atom by Al are very small. The direct gap at Γ becomes larger, and degenerate states at high-symmetry directions split because of the differences in the potentials of Ga and Al. The SL spectra contain a few extra peaks; but they still exhibit all the structure elements characteristic for zinc-blende semiconductors. The effects of the zone-folded bands multiply of course the interband transitions and the number of k points which contribute to the peaks, but a careful analysis¹¹ shows that the summation of all interband transitions between all folded and nonfolded bands which contribute to the common peaks have their equivalent counterparts in the zinc-blende BZ.^{9,20} Further, the calculations show that the SL spectra for the two polarizations are very similar, except that $\epsilon_2^\parallel(\omega)$ have somewhat higher¹¹ peak

TABLE I. Calculated and experimental values of band gaps (E_g) at Γ , spectral positions (in eV) of peaks in $\epsilon_2^\perp(\omega)$ for the $(\text{GaAs})_m(\text{AlAs})_n$ superlattices and bulk GaAs and AlAs, and interband static dielectric constant. The last line gives the average-medium values (obtained by our averaging the inverses of ϵ_0 of bulk GaAs and AlAs).

(m,n)	(1,1)		(1,2)		(2,1)		(2,2)		(3,3)		GaAs		AlAs	
	Theor.	Expt.	Theor.	Expt.	Theor.	Expt.	Theor.	Expt.	Theor.	Expt.	Theor.	Expt.	Theor.	Expt.
E_g	1.93	2.05 ^a	2.03	2.10 ^b	1.74	1.82 ^b	1.85	2.02 ^a	1.79	...	1.51	1.43 ^c	2.96	3.02 ^d
E_0	2.04	2.07 ^e	2.20	2.37 ^e	2.06	1.85 ^e	2.20	2.08 ^e	2.15	2.07 ^e	1.51	1.43 ^c	3.04	3.02 ^d
E_{SL}	3.15	...	3.00	...	3.00	...	2.96	3.02 ^e
E_1	3.22	3.20 ^e	3.50	3.37 ^e	3.26	3.08 ^e	3.36	3.25 ^e	3.33	3.25 ^e	3.16	2.92 ^c	3.82	3.90 ^d
E_{1s}	3.50	3.40 ^e	...	3.59 ^e	...	3.28 ^e	...	3.45 ^e	...	3.48 ^e	3.38	3.14 ^c	4.05	4.05 ^d
E_2	4.65	4.67 ^e	4.65	4.63 ^e	4.68	4.67 ^e	4.67	4.64 ^c	4.69	4.60 ^c	4.83	4.96 ^c	4.73	4.69 ^d
E'_{SL}	5.00	4.90 ^e	4.80	4.86 ^e	4.80	...	4.90	4.96 ^e	4.83	4.98 ^e
E'_1	5.70	...	5.64	...	5.67	...	5.70	...	5.70	...	5.60	6.20 ^f	5.51	...
ϵ_0^\perp	9.12	...	9.99	...	11.60	...	10.93	...	12.01	...	12.95	10.9 ^g	10.17	9.1 ^g
ϵ_0^\parallel	9.17	...	10.03	...	11.73	...	10.96	...	12.38	...	12.95	10.9 ^g	10.17	9.1 ^g
$\langle \epsilon_0 \rangle$	11.39	...	10.95	...	11.83	...	11.39	...	11.39	...				

^aIshibashi *et al.*, Ref. 12 (4 K). For other luminescence data see Refs. 13 and 14.

^bNagle *et al.*, Ref. 15 (4 K).

^cLautenschlager *et al.*, Ref. 16 (300 K).

^dGarriga *et al.*, Ref. 17 (300 K).

^eGarriga *et al.*, Ref. 1 and present work (300 K).

^fPhilipp and Ehrenreich, Ref. 18 (300 K).

^gHarrison, Ref. 19.

intensities than $\epsilon_2^\perp(\omega)$. [This applies to the SL's with very short periods considered in the present work. For (m,n) larger than (6,6) considerable anisotropy is predicted near E_0 , in agreement with Ref. 3].

We shall now discuss the SL-specific features of the dielectric functions. Figure 1 shows the appearance of two new peaks, labeled E_{SL} and E'_{SL} . The absence of these in the bulk materials may be seen from the calculations in Ref. 9. The E_{SL} shoulder appearing below the E_1 peak is attributed to transitions near the point where the ΓL direction cuts through the surface of the tetragonal SL BZ. In the (1,1) SL, E_{SL} is absent because the high-symmetry L point of the zinc-blende BZ coincides with the R point of the tetragonal BZ. The E'_{SL} shoulder is related to parallel-band transitions along the ΓX direction and transitions between folded bands near ΓZ . The structure labeled E'_1 is not present in the ellipsometry spectrum because of the limitation in photon energy. (With respect to the omission of the peak E_{1s} , see Ref. 4). Concerning the shift in energy with the SL period, we consider first the cases with $m=n$. These show (Table I) that the low-energy optical peaks E_0, E_{SL}, E_1 and the higher-energy peak E'_{SL} shift to lower energies as the period of the SL increases, in good agreement with the experimental observations. Next, the data for the two cases with different m and n show that E_1 lies 0.24 eV (0.30 eV, experimentally) higher in $(\text{GaAs})_1(\text{AlAs})_2$ than in $(\text{GaAs})_2(\text{AlAs})_1$. This may be understood from the difference in the relative amounts of AlAs and GaAs in the two cases, and the shifts reflect that E_1 is higher in energy in AlAs than in GaAs. For all five SL's the calculated spectral position of E'_1 is almost the same, 5.64–5.70 eV; i.e., neither for $m=n$ nor for the SL's with different compositions does this peak shift when the period is changed. This reflects the fact that the initial, as well as final, states for these transitions have approximately equal amplitudes in the GaAs and AlAs regions, and since this structure is located at nearly the same energy in the two bulk compounds, it is not affected by the formation of the SL.

The main peak in ϵ_2 has been labeled E_2 because of its similarity with E_2 in the bulk semiconductors, and the structure element at slightly higher photon energy is called E'_{SL} because it looks like a new structure appearing in the SL. In fact we associated both with E_2 -type transitions; their origins in k space almost coincide.¹¹ In the (1,1) SL it is impossible to associate states to either the "AlAs" or the "GaAs" side. In that case the occurrence of two E_2 peaks reflects the band splittings caused by the perturbation introduced by the difference between the Al and Ga potentials. For (m,n) larger than (1,1), E_2 remains stationary at 4.67 eV (very close to the bulk-AlAs value), whereas E'_{SL} is stable with respect to the period in the narrow range 4.80–4.90 eV, i.e., near the bulk GaAs E_2 peak position. These observations apply to the theoretical as well as the experimen-

tal data. For (m,n) larger than (1,1) there is at least one As layer that can be associated with the "Ga side" and one that can be considered as belonging to the "Al side." It is tempting to assume that the stationarity of the two peaks reflects the case that one is due to transitions from As- p states to As- s,d states occurring on the As atoms on the Al side, and the other is due to transitions essentially taking place on the GaAs side. We have examined the wave functions of the states responsible for these structures for the (2,2) SL, but did not find any evidence of confinement that could support such a hypothesis.

The E_0 energy which gives the onset of the absorption edges in the optical spectra does not, for all SL's, coincide with the minimum energy gap (E_g in Table I) at Γ because the dipole matrix elements for the direct transition to a zone-folded state at Γ are very small as compared to an allowed direct transition, $\Gamma_8^v \rightarrow \Gamma_6^c$, in the bulk zinc-blende compounds.

The theoretical spectrum (dotted curve in Fig. 1) contains weak structures that disappear as the broadening (solid curve) is included. One example is indicated by an arrow without a label. Corresponding structures could not safely be identified in the experimental data.

The interband contribution to the static dielectric constant ϵ_0^j ($j = \perp, \parallel$) can be evaluated with the sum rule

$$\epsilon_0^j = 1 + (2/\pi) \int_0^\infty \omega^{-1} \epsilon_2^j(\omega) d\omega. \quad (1)$$

The results²¹ are presented at the end of Table I, together with the theoretical and experimental values of the static dielectric constants¹⁹ of bulk GaAs and AlAs. The calculated ϵ_0^j increases with SL period, and ϵ_0^\parallel is slightly greater than ϵ_0^\perp , but their difference is very small. Since the dielectric constants of bulk GaAs and AlAs are different, ϵ_0^j of the SL's may be expected to depend on the relative amounts of Ga and Al as in the case of $\text{Al}_x\text{Ga}_{1-x}\text{As}$ alloy, but an average-medium model cannot explain the different values for $(\text{GaAs})_m(\text{AlAs})_m$ when m goes from 1 to 3. This rather shows that each ultrathin SL behaves like a new crystal with its own dielectric properties, different from what would be predicted by a macroscopic averaging scheme (bottom line of Table I).

In conclusion, the calculated optical properties of GaAs-AlAs SL's derived from self-consistent band structures agree well with ellipsometric measurements. Two new peaks were found in the dielectric functions of the SL's. One, E_{SL} , is induced by the tetragonal symmetry for SL's where at least one of the constituent layers is wider than one monolayer. Another (E'_{SL}) is like the main peak (E_2) considered to have similar origin as E_2 in the bulk zinc-blende compounds, but the occurrence of such two peaks is specific to the SL's. All other peaks have their counterparts in the bulk materials. Apart from one structure (E'_1), which was not included in the

experimental spectra because of the finite photon-energy range, a one-to-one⁴ correspondence is established between the calculated and experimentally found prominent structure elements. The anisotropy effects, as expressed in terms of the polarization dependence of the dielectric functions, are shown to be very small in contrast to an earlier calculation.² It would therefore be interesting experimentally to examine the polarization dependence of the optical properties.

¹M. Garriga, M. Cardona, N. E. Christensen, P. Lautenschlager, T. Isu, and K. Ploog, *Phys. Rev. B* **36**, 3254 (1987).

²E. Caruthers and P. J. Lin-Chung, *Phys. Rev. Lett.* **38**, 1534 (1977), and *Phys. Rev. B* **17**, 2705 (1977).

³H. Kamimura and T. Nakayama, in *Proceedings of the Eighteenth International Conference on the Physics of Semiconductors, Stockholm, Sweden, 1986*, edited by O. Engström (World Scientific, Singapore, 1987), p. 643.

⁴Our calculated spectra includes the relativistic effects except the spin-orbit coupling. Therefore, in contrast to the experimental spectra, ours do not contain the peak E_{1s} ($E_1 + \Delta_1$). A calculation for the (1,1) SL with spin-orbit coupling (M. Alouani, S. Gopalan, and N. E. Christensen, to be published) shows that this structure element appears in agreement with the measurement.

⁵O. K. Andersen, *Phys. Rev. B* **12**, 3060 (1975).

⁶P. Hohenberg and W. Kohn, *Phys. Rev.* **136**, B964 (1964); W. Kohn and L. J. Sham, *Phys. Rev.* **140**, A1133 (1965).

⁷N. E. Christensen, *Phys. Rev. B* **30**, 5753 (1984).

⁸G. B. Bachelet and N. E. Christensen, *Phys. Rev. B* **31**, 879 (1985); N. E. Christensen, *Phys. Rev. B* **37**, 4528 (1988).

⁹M. Alouani, L. Brey, and N. E. Christensen, *Phys. Rev. B* **37**, 1167 (1988).

¹⁰O. Jepsen and O. K. Andersen, *Solid State Commun.* **9**, 1763 (1971).

¹¹Alouani, Gopalan, and Christensen, Ref. 4.

¹²A. Ishibashi, Y. Mori, M. Itabashi, and N. Watanabe, *J. Appl. Phys.* **58**, 2691 (1985).

¹³D. S. Jiang, K. Kelting, T. Isu, H. J. Queisser, and K. Ploog, *J. Appl. Phys.* **63**, 845 (1988).

¹⁴E. Finkman, M. D. Sturge, M.-H. Meynadier, N. E. Nahory, M. C. Tamargo, D. H. Hwang, and C. C. Chang, *J. Lumin.* **39**, 57 (1987).

¹⁵J. Nagle, M. Garriga, W. Stolz, T. Isu, and K. Ploog, *J. Phys. (Paris) Colloq.* **48**, C5-495 (1987).

¹⁶P. Lautenschlager, M. Garriga, S. Logothetidis, and M. Cardona, *Phys. Rev. B* **35**, 9014 (1987).

¹⁷M. Garriga, P. Lautenschlager, M. Cardona, and K. Ploog, *Solid State Commun.* **61**, 157 (1987).

¹⁸H. R. Philipp and H. Ehrenreich, *Phys. Rev.* **129**, 1550 (1963).

¹⁹W. A. Harrison, *Electronic Structure and the Properties of Solids* (Freeman, San Francisco, 1980).

²⁰J. R. Chelikowsky and M. L. Cohen, *Phys. Rev. B* **14**, 556 (1976).

²¹When our calculated values are compared to experiments it should be borne in mind that many-body effects not included in the theory here are expected to modify the results; see discussion and references in Ref. 9.